Analysis and Optimisation through Mathematical Modelling: Muresk Farm Photovoltaic Reverse Osmosis Water Treatment Plant

ELECTRICAL POWER ENGINEERING (HONOURS)
RENEWABLE ENERGY ENGINEERING (HONOURS)

Clinton Young

Supervisor: Martin Anda

2020

Authors Declaration

I declare the contents of this thesis are my own original work and that to the best of my knowledge this thesis contains no material previously published other persons except where citations have been made.

Abstract

Photovoltaic reverse osmosis water treatment units can be deployed into remote regions to provide remote communities with a clean water source without the need for on site electricity supply to operate. Optimisation of these units has the potential to maximise the output of purified water and to improve the overall effectiveness of the PVRO unit once it has been deployed. The aim of this project is to develop a mathematical model for the optimisation of the Muresk PVRO unit. This is achieved using a local monitoring system that can log the operational data of the PVRO unit and utilising this data to validate and tune a Microsoft Excel based mathematical model of the Muresk PVRO unit.

In this project an ESP32 microcontroller running an Arduino program was used to log the electrical and water flow data from the PVRO unit to a ThingSpeak IOT portal and a local SD card. A mathematical model of the Muresk PVRO system was developed, and two months of data were compared with the data from the monitoring unit to tune and validate the model. With the model tuned the mathematical model was used to investigate optimising the PVRO output by adjusting the tilt angle of the solar array. By increasing the array tilt from 30 degrees to 45-degrees the daily minimum output improved by 9% with a marginal loss of 1% to the annual water output. This increases the suitability of the unit to applications where a consistent output of clean water is more desired than just maximising the annual output.

Table of Contents

Table of Figures

Acknowledgments

I would like to thank the following people for the assistance with this project:

Glossary of Terms

AC – "Alternating Current" is where electrical current periodically cycles between both directions

DC – "Direct Current" is where the electrical current flows in a fixed direction

IOT – "Internet of Things" refers to devices that connect to the internet for the exchange of data

PV – "Photovoltaic" refers to the conversion of light to electricity

PVRO – "Photovoltaic Reverse Osmosis" is a solar powered reverse osmosis used to purify water in remote locations

SOC – "State of Charge" is a percentage value representing the amount of available power in the battery

DoD – "Depth of Discharge" is a percentage value representing the amount of power taken from the battery

RO – "Reverse Osmosis" refers to a water purification process utilising a semi-permeable membrane

Introduction

The purpose of this project is to first analyse the unit's operational data through long term monitoring. Then using this data, establish a mathematical model of the unit to allow simulation of the PVRO unit in a variety of operating conditions, changing the configuration and location to determine how the unit performs under these varying conditions. Through simulation we can instantly see in detail how the unit would perform under the varied conditions and hence optimise the dispatch of these units into different remote areas.

89Km from Perth just south of Northam is the Muresk Institute, an education and training facility for the Western Australian agricultural sector. Through joint work between Murdoch University and Moërk Water Solutions, a small PVRO pilot plant was installed at the Muresk Institute for testing the use of these units in the Wheatbelt. The PVRO unit utilises a fixed solar array and a small battery set to power a reverse osmosis unit. The reverse osmosis unit takes water from a nearby bore, filters and purifies it to produce clean water as an output. These units can be placed in remote locations to provide a reliable source of clean water without the need for on-site power. The Muresk PVRO unit is used as the basis of the model for this project.

Objectives

The aims of this project break down into 5 key areas:

- ➢ Develop a monitoring system to log the operational data of the Muresk PVRO unit.
- ➢ Develop a mathematical model of the Muresk PVRO unit to be used in a simulation of the real-world PVRO unit.
- ➢ Utilise the operational data from the monitoring system to tune and validate the mathematical model.
- ➢ Utilise the mathematical model to optimise the Muresk PVRO unit through simulations.
- ➢ Utilise the mathematical model to determine how the Muresk PVRO unit would perform in varying locations and operating conditions.

Literature Review

Background

Water is an essential resource for any community across the globe. Approximately one quarter of the world's population lacks access to adequate amounts of clean fresh water [1]. This is a challenge in remote and developing areas where it is often unviable to implement large-scale water decontamination and storage [2]. Small scale desalination (100 m3 /day or less) [3] provides flexibility in converting the local lower quality water supplies into a high-quality drinkable water. Renewable powered desalination technology such as Photovoltaic reverse osmosis (PVRO) is an attractive possibility in decentralized, off-grid communities with brackish water sources. PVRO combines an array of photovoltaic (PV) cells powering a reverse osmosis unit to provide a consolidated method of water desalination.

Reverse Osmosis

Reverse osmosis (RO), used in more than 80% of the desalination plants in the world, has become a common method of water purification [4]. External pressure is applied to the untreated, high-solute water to reverse the natural process of osmosis through a semipermeable membrane [5]. This pushes the pure water component of the untreated input water, to the other side through the membrane. This results in a purified 'permeate' water output and a secondary concentrated waste water 'brine' output. The potential of reverse osmosis to reject up to 99% of all ionic solids [5], allows for a high quality water output, thereby allowing for a wide variety of water input sources including seawater and brackish water sources.
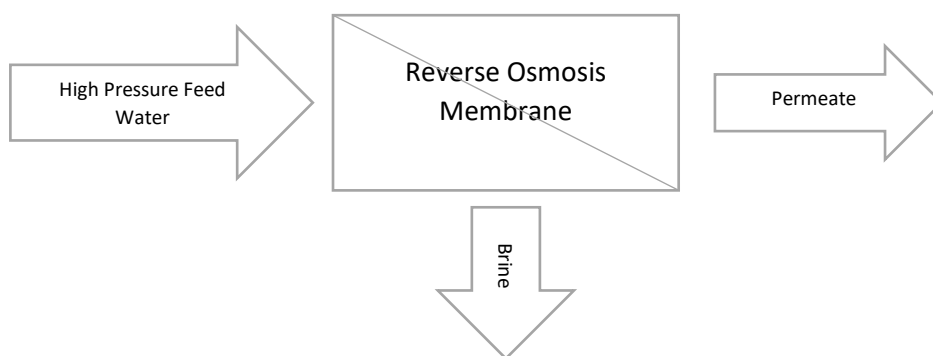
Figure 1: Basic reverse osmosis process

Utilizing RO as the primary method of purifying water is becoming more popular as the relative costs decrease. For coastal communities the most abundant source of water is seawater which is high in concentrated salts and impurities but on a small scale, RO feedwater can be improved by utilizing "beach wells" [4]. When reverse osmosis is utilized for seawater desalination the technology is superior to older thermal desalination methods," it is more effective than thermal desalination, with lower energy requirements, lower operating temperatures, and lower water production costs" [3].

The process is still very energy intensive and "high energy consumption and potential environmental impacts are the main challenges" [3]. For inland communities, alternate brackish water sources are often available, but water quality is a major issue and, in many cases, cannot be used for drinking without first removing the contaminants. When brackish water supplies such as rivers or groundwater are used, due to the reduced concentration of salts relative to seawater, lower pressures are required for the reverse osmosis unit lowering energy costs further.

Remote Solar / Battery System

Solar energy is a readily available energy source that comprises all energy received by the earth from the sun. Photovoltaic (PV) systems contain cells that directly convert sunlight into electricity [6]. PV cells typically consist of layers of semi conductive materials. When sunlight shines on the PV cell, the photons hitting the upper layer "knocks" electrons into the lower layer causing electricity to flow. PV cells have no moving parts and hence incur no operating and low maintenance costs. Utilizing the suns energy is a passive renewable energy source.

Current PV cell technology includes monocrystalline cells, polycrystalline cells and amorphous silicon. Monocrystalline cell technology is widely used due to high efficiency of more than 20%. The cells consist of large silicon single-crystals which have been doped to form n-type or p-type silicon [6]. Polycrystalline cells are traditionally cheaper than monocrystalline cells but with lower efficiencies. The cells consist of crystallized silicon in a fixed direction and are cut from a larger block [6]. Amorphous silicon is a thin film technology with a relatively low efficiency but requiring fewer material to manufacture thus reducing costs. The cells utilize silicon in non-crystalline form in disordered structure [6].
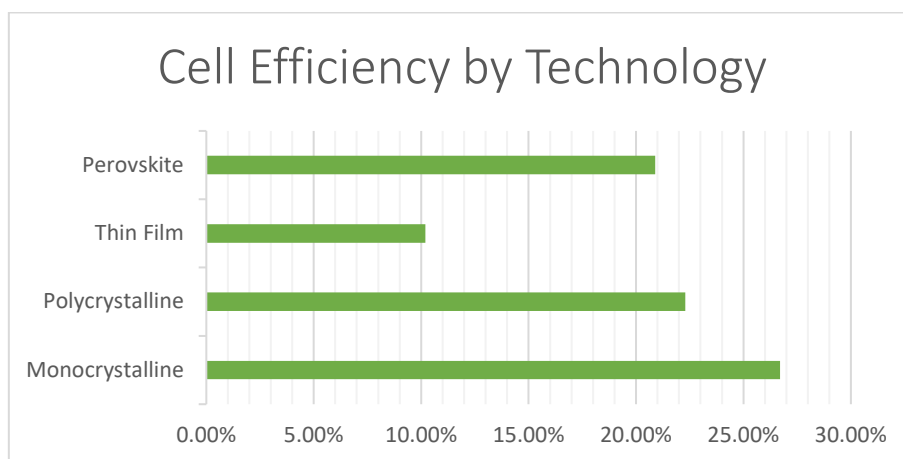
Figure 2: Solar cell efficiency by technology [7]

Ongoing developments in cell technologies include bifacial cells which allow for the conversion of sunlight which is reflected onto the back side of the panel, improving energy yield by 15-20% per year over standard cells [8]and perovskite cells showing potential for low cost, high performance cells with "rapid advances in efficiencies of perovskite PV cells from 3.81 % to 23.7 % in just 9 years" [9]. Solar PV power has undergone rapid growth in recent years to become a major source of renewable energy accounting for 1.7% of global electricity generation [10]. Solar PV has also experienced a rapid reduction in cost from $4 per watt in 2007 to $0.35 per watt in 2017 [10].

The utilization of solar energy to power the system allows the unit to be placed in remote areas where grid electricity may not be available, or grid connection is not feasible. RO relies on a continuous energy source for its operation as the RO membrane requires constant pressure to maintain permeate flow. As the nature of solar radiation is highly variable, PVRO plants typically utilize a battery system as either an energy buffer or for backup. With the inclusion of a battery in the system, the batteries have been shown to "perfectly decouple the solar panel and the RO unit" [11].

Battery storage systems have seen similar growth to that of solar PV systems. The two major battery technologies currently in use are Lead-Acid and Lithium-Ion batteries. Lead-Acid batteries are an old technology but are still the most common option worldwide for the storage of electricity [12]. Lead acid batteries are comparatively large and heavy due to the batteries construction which consists of lead plates immersed in an electrolytic solution of sulphuric acid [12]. Variants of the standard "flooded" lead acid battery include valve regulated lead acid (VRLA) batteries utilizing a valve to regulate the release of hydrogen gas from the cell increasing battery lifespan, absorbed glass mat (AGM) which add an internal matting to suspend the electrolyte close to the lead plates allowing for deeper cycling and Gel batteries which add silica gel to the electrolyte causing it to stiffen allowing even deeper battery cycling.

Lithium ion batteries are a more recent battery technology that has seen many recent developments which have accelerated since the emergence of the electric vehicle industry. Lithium Ion batteries have longer lifespan, higher efficiency, faster charge/discharge capabilities and a lighter more compact form factor than lead acid batteries [12]. The downside of the newer technology is the cost per watt hour is at least twice that of lead acid batteries, but that is expected to improve significantly over the next few years [12].
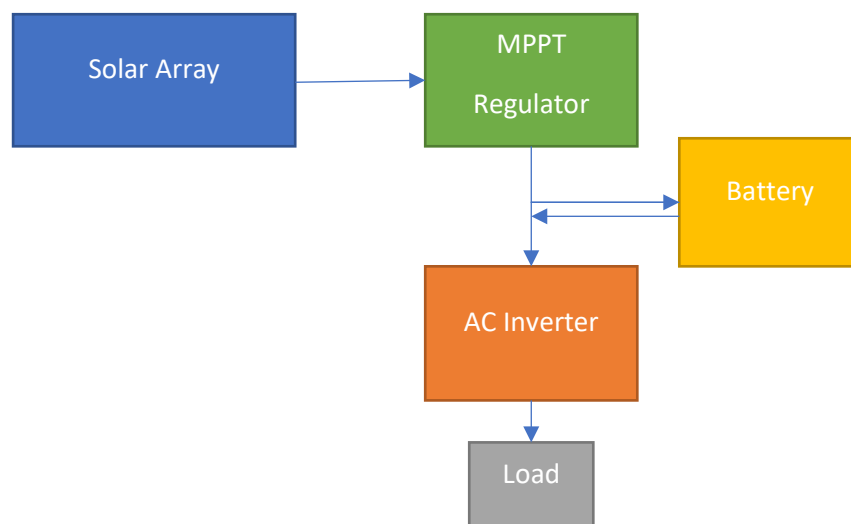

Figure 3: Typical Remote Solar Battery System Layout

Remote Monitoring of PVRO System

Data acquisition in modern society is getting easier with the rise smaller cheaper computers that can be embedded in just about anything. "From the year 2014, embedded systems and wireless data transmission have been increasingly implemented for PV plants and meteorological variables monitoring, instead of using commercial dataloggers" [13]. The Internet of Things (IOT) is a system incorporating microcontrollers that are connected to the internet either directly through ethernet, cellular modems or indirectly through Wi-Fi, Bluetooth or LoRa networks connecting to a central "hub" that relays the data to the internet [14]. This internet connection allows these "smart" devices to upload information to a cloud server and be controlled over the internet. This allows real time monitoring of data and downloading all logged data from any computer connected to the internet. This method of collection is a much easier method of data collection over traditional dataloggers which require the unit to be directly connected to a computer to access the recorded data especially when it comes to remote systems where physical access can be difficult. Logging methods proposed by the IEC standard IEC61724 which covers PV system performance monitoring recommend a maximum sampling interval of 1 minute and a maximum recording interval of 15 minutes for medium accuracy and 60 minutes for basic accuracy [15].

IOT systems require some form of microcontroller to process the data from the sensors and forward the data to the online IOT platform. There are many microcontrollers capable of doing this, a few popular examples include the ESP-series modules, Arduino and Raspberry Pi.

The most common ESP-series module is the ESP8266, a well-known Wi-Fi solution among hobbyists and students [16]. It features integrated Wi-Fi working on common 802.11 b/g/n protocol, 1 MB of flash memory, nine general-purpose input/output (GPIO) pins supporting serial-peripheral interface (SPI) and inter-IC (I2C) communication protocols [16]. The ESP32 is an upgraded version featuring both Wi-Fi and Bluetooth alongside a faster 160Mhz dual-core processor and a wider variety of input pins [16]. Arduino offers a vast range of open-source boards with a wide variety of specifications to choose from and an active online community for software support [16]. For IoT applications, the Arduino Yun features onboard 802.11 b/g/n Wi-Fi, ethernet and micro-SD card slot [16].

Alternatively, Arduino also offers the Genuino MKR1000, featuring a Li-Po charging circuit and a Cryptochip for secure communication [16]. Raspberry Pi is more of a "single-board computer" than a microcontroller featuring a quad-core processor, an onboard graphics processing unit, Wi-Fi, ethernet, USB ports, micro-SD card slot and a HDMI output [16]. However, additional hardware is required for interfacing with analogue inputs and despite a similar supportive online community to Arduino, the learning curve can be much steeper [16].

With the microcontroller processing the data, this information is then forwarded to an IOT platform. "An IoT platform is a complete suite of services that facilitates services like development, deployment, maintenance, analytics as well as intelligent decision-making capabilities to an IoT application" [17]. Some examples include the Google Cloud Platform running on Google's infrastructure, ThingWorx designed to build and run the connected world and ThingSpeak featuring MATLAB data analytics and visualization [17]. Many more IOT platforms exist with a variety of features ranging from data visualisation to intelligent control systems.
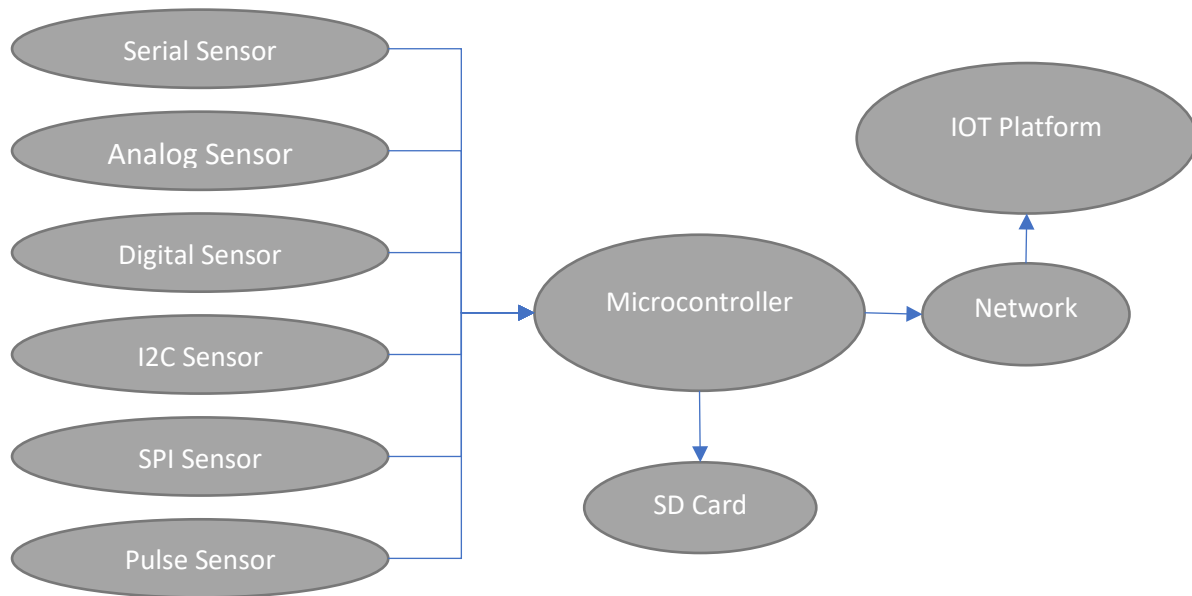
Serial Sensor

Analog Sensor

Digital Sensor

I2C Sensor

SPI Sensor

Pulse Sensor

Microcontroller

IOT Platform

Network

SD Card

Figure 4: IOT Data Acquisition Layout

Data Acquisition

The basic data required for monitoring the PVRO system comes from three major components of the system, the solar array, the battery and the RO unit. The solar array data consists of the dc current and voltage of the solar array providing information on the power input of the system. The battery data consists of the battery voltage, current and state of charge (SOC) giving an indication on how well the energy storage is being utilized. The key data from the RO unit is the input AC voltage, current and the output pure water flow rate giving an indication of the performance of the RO unit. Collecting the data required to properly monitor the PVRO system can be achieved in a variety of ways split into two main categories, invasive and non-invasive. Invasive techniques involve sensors that are placed within the system requiring some modification to the system for correct installation and to obtain data, sometimes these techniques have an impact on system performance. Non-invasive techniques alternatively provide data collection without modification to the existing system but can be significantly more expensive.

For the measurement of electrical current the techniques are well established including shunt resistors or magnetic transducers [18]. Shunt resistors are a widespread and inexpensive method but are both an invasive technique requiring the shunt to be placed in series with a power conductor and suffers an error on accuracy higher than 5% [18]. Alternatively, magnetic transducers such as current transformers or hall-effect sensors can be utilised. Current transformers (CT) are used to measure AC currents due to the required changing magnetic field to induce a current, this is a non-invasive method that clamps onto one current carrying conductor causing a smaller proportional current to flow through the CT. This current can then flow across a precision resistor to obtain a proportional voltage signal [19]. Hall effect sensors unlike CTs can measure both AC and DC currents but require an additional integrated circuit (IC) to take measurements. For the measurement of voltage, the simple approach is direct measurement which can be considered invasive due to a minimal impact on the existing system, for high voltage measurements transformers or voltage dividers can be used to step down the voltage to safer, easily measurable levels. Currently there is no commercially available non-invasive sensor that can measure the AC voltage however capacitive

coupling, an experimental technique that involves placing a cylindrical conductor around each AC conductor shows potential for a low cost, non-invasive solution [18].

Modern solar battery systems include a maximum power point tracker (MPPT) regulator to maximise solar output, an AC inverter to convert the DC power into AC power and usually some form of battery monitor for the monitoring and protection of the battery unit. These existing MPPT regulators, AC Inverters and if fitted, the battery monitors all can measure their own internal power flows. In the case of the Victron units used in the Muresk PVRO system there is an open source serial communication interface that by default sends out data every second containing the information obtained by the unit [20]. In the case of the MPPT unit this data includes the solar MPPT voltage/current, the load voltage/current, the battery voltage/current as well as historical information such as daily energy yield and unit operating status [21]. In the case of the AC inverter, the data includes input DC voltage/current, output AC voltage/current and other system status information [22]. If the battery monitor is fitted, detailed information on the battery can be collected, including battery voltage/current, SOC, consumed Ah and a variety of historical data including min/max voltage, number of cycles, deepest discharge, previous DoD and amount of charged/discharged energy [23]. All this data can be directly interfaced with a microcontroller serial port configured to 19200 baud rate [20], providing extensive amounts of system data, while remaining completely non-invasive.

For measuring water flow rate many techniques exist. An example of an invasive method is a turbine flow meter which utilizes the water flow to cause a turbine to rotate. A magnetic sensor is used to detect the speed the turbine is spinning by outputting a pulse rate proportional to the flow rate. Non-invasive methods such as ultrasonic sensors utilizing high frequency waves to detect the flowrate have the advantages of simpler installation, no impact on the system and no moving parts [24].

Modelling PVRO System

Modelling of any PV system requires local weather data, particularly the solar irradiance data, as well as the efficiency of all electrical components. The calculation of energy produced by the PV array depends on the time step of the weather data used, hence weather data with finer steps would allow for more accurate simulation with finer steps [25]. Historical weather data is averaged and used to predict probable future weather data. Solar output is dependent on irradiance which can be converted to hourly data using the equation in figure 5. Temperature data can be utilized to estimate the PV cell temperature and apply a correction factor obtained from the manufacturer's datasheet (figure 6). There are many more detailed mathematical models for predicting the solar irradiance output of solar offering higher accuracy, but these methods greatly complicate the mathematical model and require additional unknown variables creating potential sources of error.

The MPPT and inverter efficiency vary depending on the load they are working at. This information may be obtained from the manufacturer's datasheet as an efficiency curve in terms of input power and rated power [25]. If unavailable, this is estimated. Battery charging and discharging losses must also be considered, but this information is usually unavailable from datasheets and must be estimated.

$$Hd^t = Isc(\sin\sigma\sin\varphi + \cos\sigma\cos\varphi\cos\omega)$$

$Hd^t = Irradiation\ on\ tilted\ surface$

σ = Declination Angle (degrees)

$\varphi = Lattitude$ (degrees)

Isc = Solar constant (Wm^{-2})

$\omega = Hour\ angle$ (degrees) $= 15(12 - t)$

t = true solar time (hours)

$$Pout = Pin * Efficiency$$

Peffective = Pnominal - (Ptc * T)

P = Power (W)

Ptc = Solar power temperature coefficient (W/℃)

T = temperature (℃)

Figure 5: Solar irradiation hourly calculation formulae [28]   Figure 6: Power efficiency and temperature compensation formulae

For the modelling of PVRO systems which include battery storage, a method of estimating the batteries SOC must be utilized. Many methods exist for determining the battery SOC, including discharge test, voltage-based examination, coulomb counting, Kalman filtering and neural network [26]. Voltage based monitoring uses the batteries terminal voltage to estimate the battery SOC, it is a simple method, but requires the battery be disconnected from the load or "rested" for a period before taking a reading. This method may not be very accurate but can be improved by measuring temperature and applying a compensation factor. Coulomb counting involves measuring the battery current and integrating it over time, this method suffers from the SOC "drifting" over time and must be calibrated/reset periodically [26]. This method allows real time SOC without disconnecting the battery from the load.

The RO unit is the main load in the system, but some systems have auxiliary loads such as lighting or cooling fans. The RO unit power draw comes mostly from the high pressure feed pump plus a smaller power draw from the feed pump. The pump shaft power can be determined by the feed flow rate, the pump pressure and the pump efficiency [27]. In the case of Muresk PVRO unit there is plans for an external mixing unit that draws a significant amount of power from the system. To accurately model battery levels this load plus all auxiliary loads must be considered in the model.
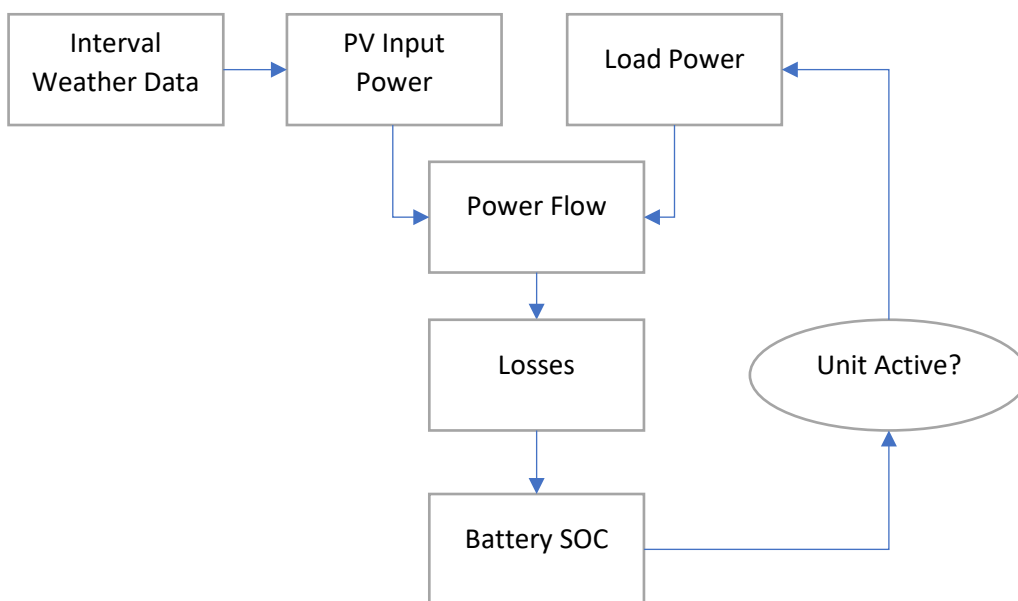
Figure 7: Simplified model block diagram of PV battery system simulation

Utilizing the input irradiance data, the resultant solar input power can be calculated and hence all subsequent energy flows. Accounting for all energy flows, and the efficiencies of individual components the resultant time the unit is active can be determined and hence the permeate water output can be calculated. The resultant system can then be represented by a mathematical model that can be calculated through a MATLAB program or iteratively through a Microsoft Excel spreadsheet providing interval data for all parameters. Once significant amounts of data have been obtained from the data monitoring of the Muresk PVRO unit this data can then be compared to the simulated model to both verify and improve the accuracy of the model.

Methods

This project can be broken down initially into two main parts; the data acquisition stage and the modelling stage. The data acquisition stage requires setting up a monitoring system on the remote PVRO system. The initial priority is to set up the monitoring unit to maximise the amount of logged data available for later use. Once this is done data logging will run in the background while the second stage of the project, the modelling stage, is being worked on. In this stage a theoretical model is established to simulate how the unit is expected to run. Once these two stages are complete the final stage of the project is to combine the data from the monitoring stage into the theoretical model to increase the accuracy of the model and to increase the usability of the model.

Data Acquisition Stage

Development - Overview

The monitoring system must be capable of measuring the key parameters of the PVRO system. In the Muresk PVRO system these are the solar power, battery power, inverter power and the RO input/output flowrates. To achieve the monitoring of these systems, a microcontroller-based system was chosen to better integrate into the unit than a standard datalogger and to add some flexibility to accessing the data. Already being familiar with microcontroller programming and interface circuit design made this method more favourable.

Figure 8: Muresk PVRO Unit, Exterior (left), RO Unit (middle), Power Board (right)

To determine compatibility of the monitoring system, the components of the Muresk PVRO unit needed to be analysed. The Muresk PVRO unit consisted of 500L/hr RO unit powered by 4.3kW of solar panels and a 48V 100Ah lead acid battery system. Inside the unit the electrical system consisted of a Victron MPPT solar regulator, a Battery Management System (BMS) and an Inverter which fed 240V AC power to the RO unit and a cooling fan. The Victron MPPT and BMS units on further investigation were both compatible with Victron's VE.Direct protocol, providing serial output of all internal data. The RO unit power was fed through a single AC cable. The water inlet and outlet pipes used 25mm BSP threaded fittings on the inlet and outlets.

Figure 9:PVRO Basic Electrical Layout

Development - Sensors

For measuring the DC voltages and currents the existing VE.Direct data could be utilized or external current and voltage sensors could be utilised. The VE.Direct data was used as it was both the simplest method to obtain the data and the least invasive. The low sample rate isn't an issue due to the long measurement period and the mV accuracy enough for this application.

	SAMPLE RATE	ACCURACY	DIFFICULTY	INVASIVE
VE.DIRECT DATA	1S	mV	Low	Low
EXTERNAL SENSOR BOARD	<1mS	uV	Moderate	High

Figure 10: DC voltage measurement method comparison

For measuring the AC voltage and currents the only option available was to implement some external sensors due to the Inverter not being VE.Direct compatible. The chosen method was to use current clamps on the AC cables to obtain current and to assume a fixed voltage of 240V. This method is very simple in comparison and safer than trying to measure AC voltages. The voltage divider with current shunt method would require more interface circuitry and be much more invasive than the current shunt method

	V/I	SAFETY	ACCURACY	DIFFICULTY	INVASIVE
CURRENT TRANSFORMER	I	High	High	Low	Low
VOLTAGE DIVIDER + SHUNT	V+I	Low	High	High	High

Figure 11: AC voltage and current measurement method comparison

For measuring the water flowrates, a variety of flow sensors were capable of being fit to the RO unit. The key differences between the potential options listed were the complexity of the method and implementation as well as the cost of the sensor type. The chosen flow sensor was a paddle turbine flow meter being the simplest and cheapest option to implement.

	ACCURACY	COST	DIFFICULTY	INVASIVE
PADDLE TURBINE	Moderate	Low	Low	Moderate
ROTOR TURBINE	Moderate	Moderate	Low	Moderate
ULTRASONIC	High	High	High	Low

Figure 12: Flow sensor measurement method comparison

Development - Data

For recording and accessing the recorded data it was decided this system should utilize independent and redundant data recording systems to ensure the reliability of the system. These being an online IOT data portal and a local SD card as backup.

The online data portal will have the interval data uploaded, stored online and be easily accessible from anywhere. The disadvantage of an online platform is the uploading of the data relies on a local internet connection that may have outages.

Meanwhile the local SD card, having the disadvantage of requiring physical site access to access the data is also the simplest and most reliable way to record the data collected by the microcontroller.

An alternate option that was considered on top of the other systems was a microcontroller-based FTP server for accessing the data stored on the SD card. While this did solve the accessibility issues

of a simple SD card it would increase the bandwidth usage of the system and is unnecessary if the data portal is available. Similarly emailing the data periodically did allow an alternate method of retrieving the data it was less user friendly than the IOT portal while being less reliable than the SD card.

	RELIABILITY	COST	DIFFICULTY	USER FRIENDLY
SD CARD	High	Low	Low	Low
IOT PORTAL	Moderate	None	Low	High
FTP SERVER	High	Low	High	Low
EMAIL DATA	Moderate	None	Moderate	Low

Figure 13: Data recording method comparison

Connecting the data acquisition system to the online data portal requires an internet connection of some sort. Options available range from directly connecting to a local WiFi or Ethernet network, indirectly connecting to an existing internet connection via LoRa network or connecting directly to the internet via a cellular modem.

For this system there is no local WiFi or Ethernet connection available although there is an existing LoRa network at Muresk. Despite this a cellular modem was chosen instead to retain some independence of the data acquisition system and to improve the reliability of the system.

	AVAILABLE	COST	DIFFICULTY	RELIABILITY
LOCAL WIFI/ETHERNET	NA	None	Low	Moderate
LORA NETWORK	Distant	None	Moderate	Low
CELLULAR NETWORK	Yes	Low	Low	Moderate

Figure 14: Internet connection method comparison

With the internet connection set up the data is then sent to an online data portal. Fortunately, there are many different online IOT platforms capable of doing this. For this system the ThingSpeak platform was chosen due to it being free to use (with feature limitations), having friendly visual ways to present the data and integrating MATLAB analytics, allowing for processing the data.

Development - Platform

The platform for running the monitoring unit is what ties all components together and must be compatible with all every component chosen. Several options for monitoring the PVRO unit, including using the existing TrinaSolar system, a Raspberry Pi or Arduino based IOT monitoring system and a basic datalogger, can also be utilized for short term data collection.

Firstly the TrinaSolar system can directly interface with the existing TrinaSolar components used in the PVRO units solar battery system. The MPPT regulator, inverter and battery monitor all have smart electrical monitoring capability and only require a GX series control board for connecting all systems together. Unfortunately the Trinasolar GSM modem may not work in Australia due to Telstra and Optus decommissioning their GSM networks in 2016 and 2017, respectively. The other major issue with this method is the inability to add additional sensors such as flowrate sensors.

The next option is a Raspberry Pi based IOT system. The Raspberry Pi is a powerful microcontroller with wide programming options capable of IOT functionality. Raspberry Pi boards typically include WiFi and Bluetooth connectivity as well as a range of GPIO pins and compatible protocols. The main

drawback of this platform is the steep programming learning curve. Previous experience in this platform would be required for fast development of the monitoring unit.

Then there is Arduino, a simpler alternative to Raspberry Pi with a wider variety of compatible boards. Arduino isn't as powerful as Raspberry Pi, but still capable of IOT functionality. The ESP32 board is a relatively powerful microcontroller, which includes WiFi and Bluetooth capability and variety of ports such as I2C for sensor connection.

Finally an off the shelf datalogger, which is a purpose built unit typically suited for temporary monitoring and data collection. There are a wide variety of units available and compatibility with a wide variety of sensors are available some higher end models allowing for remote access to the data. Unfortunately, compatibility with the VE.Direct protocol isn't available which would require many additional sensors to replace the VE.Direct data.

It was chosen to go with the ESP32 microcontroller as a DIY IOT solution. Utilizing the Arduino platform allows for easy programming of the monitoring unit and great flexibility of the program to suit the needs of the monitoring system. An ESP32 was chosen as this board includes Bluetooth and WiFi connectivity, giving flexibility in retrieving the data. Using a WiFi Hotspot modem as an internet connection, the recorded data can be uploaded to an IOT server at 15-minute intervals providing remote access to the data. Bluetooth can allow for additional Arduino boards to be connected wirelessly providing an opportunity in expanding the boards capabilities. The ESP32 board has a range of compatible input options. The key for this project are the 30GPIO pins, the 12bit ADC, multiple UART ports and SPI interface.

Chosen Method - The DIY Monitoring Unit:

The final system was a DIY monitoring unit built around the ESP32 microcontroller. A hotspot modem provides internet connectivity to the ESP32 unit through it's WiFi connection. The ThingSpeak platform is the main data portal, allowing remote monitoring and download of the recorded data. A local SD card is added as a backup data storage in the event there is an issue with either ThingSpeak or the hotspot modem. The VE.Direct protocol feeds all data from the BMS and MPPT regulator to the ESP32 unit via its UART ports. A logic level converter was added to allow the ESP-32 compatibility with both 3.3V and 5V systems. A current transformer and interface circuitry measure the AC current out of the inverter to the system. Two paddle wheel type flow sensors measure the permeate and feed flow rates and feed proportional frequency pulses to the ESP2 through interface circuitry. The entire monitoring system is powered via a wide input buck regulator that is fed from the PVRO battery.

Parts List:
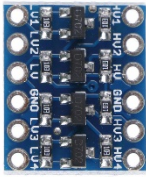
ESP-32 Dev Module		Hotspot Modem	
1" Flow Meters (FS400A)		Hologram SIM Card	
100A Current Transformer		Waterproof Project Case	
Micro SD Card Module		10A 60V-5V Buck Converter	
SD Card		Logic Level Shifter	
Capacitors/Resistors		PCB/Cable/Misc	

Figure 15: Key parts list of PVRO monitoring system

Chosen Method - Setting Up The Monitoring System

Assembly of the unit began with building the PCB, a prototype PCB with predrilled and tinned holes was chosen as the base of the unit. This method of construction offers a balance between the flexibility of breadboard and the reliability of a prefabricated, purpose-built PCB. From there the header pin sockets for connection of the ESP-32 module were soldered to the centre of the board and screw terminals at the outer edges for external connections. The buck converter, logic level shifter, micro SD card module and miscellaneous interface circuitry were installed on the PCB, near their relevant connection points to the ESP-32.

The buck converter output was set to 5V and connected to the Vin pins of the ESP-32, with a power cable connected to the buck convert input pins for the external power source. The logic level converter low side was connected to two of the hardware UART ports of the ESP-32 and two GPIO pins for software UART inputs, the high side was connected to the screw terminals. An adaptor cable connects two sets of these screw terminals to the MPPT and BMS units through their respective VE.Direct ports. The remaining two screw terminal sets remain open as spare data inputs for future expansion.

The micro SD card module was connected to one of the ESP-32 SPI interfaces and a formatted micro SD card installed. The flow meters are connected via screw terminals to the interface circuitry through to the ESP-32 GPIO pins. The current sensor is connected via screw terminals to different interface circuitry through to an ESP-32 ADC pin. The hotspot modem is powered by a female USB Type-A cable connected to the 5V buck converter output.

A program was developed to interface all components and perform the datalogging process. The basic operation of this program is to read all the input data for 15-minutes and average the data. The unit then connects to the WiFi modem, uploads the data to the ThingSpeak portal, saves a copy of the data to the SD card and repeats.

Setting up the ThingSpeak portal was relatively straightforward, with four "channels" created for receiving the monitoring unit data. The first channel is dedicated to the VE.Direct data, the relevant PV and battery data is sent to this channel with 48hr graphs displaying the data. The second channel is dedicated to the two flow sensors and the current sensor with similar graphs set to display the data. The remaining two channels were set to display the data received from the monitoring units' spare inputs. The relevant "channel keys" were added to the ESP-32 program to allow communication between the monitoring unit and the ThingSpeak portal.
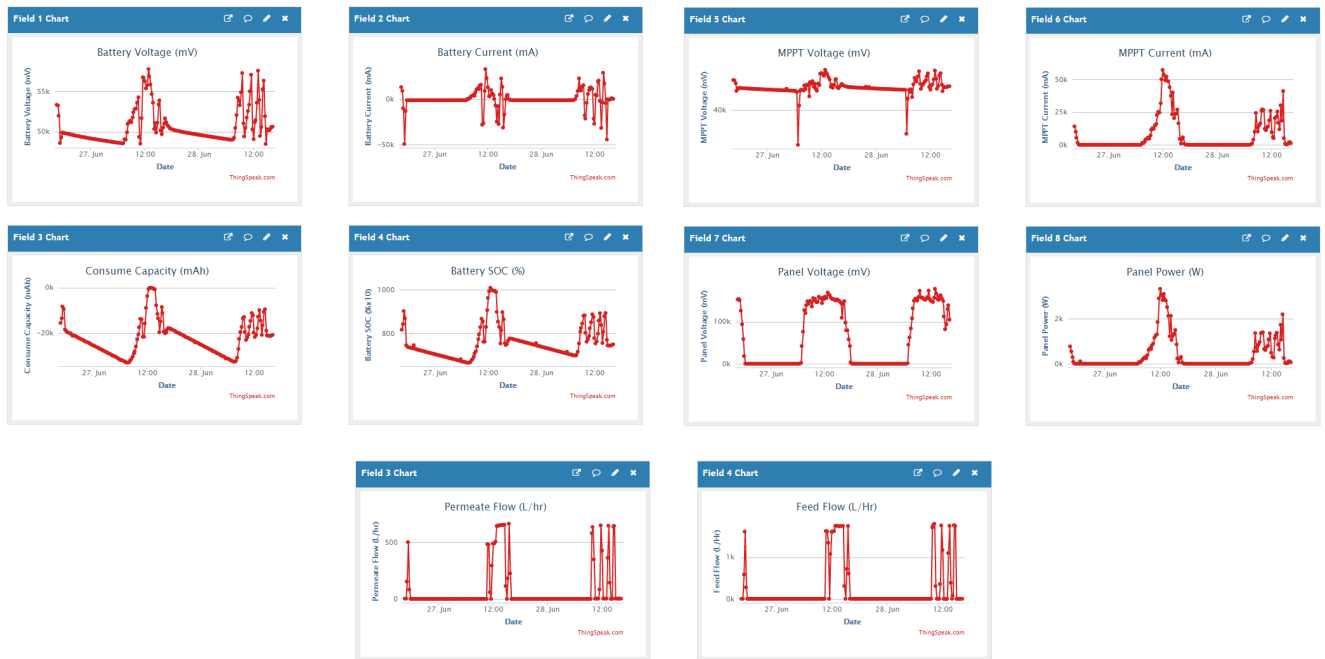
Figure 16: Setting up ThingSpeak Portal with 48hr data graphs

Physical installation of the unit involved mounting the PCB inside the waterproof case and mounting it near the electrical installation inside the PVRO unit container. The VE.Direct adaptor cables were connected to the PCB through to the MPPT module and BMS module VE.Direct ports. The flow sensors were installed inline with the RO permeate output and RO input pipes, with the sensor cables connected to the PCB screw terminals. The current transformer was installed onto the active AC cable behind the 240V AC outlet and then connected to the PCB via screw termianls. Finally, the power cable from the buck converter input was connected to the PVRO unit battery.
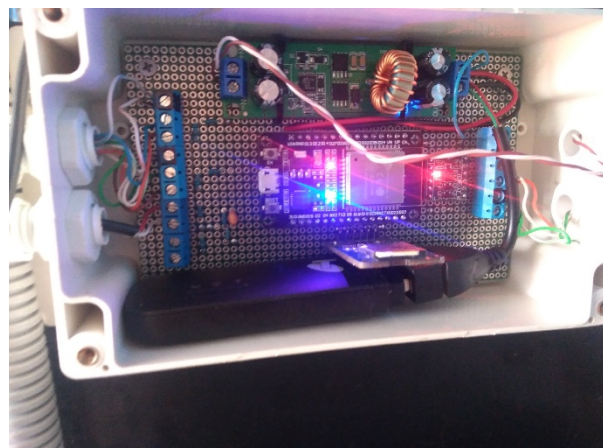
Figure 17: Assembled and installed ESP-32 based monitoring unit

Mathematical Modelling

Modelling of the PVRO system begins with defining the extent of the model and the basic breakdown of how the model is to function. All aspects of the model must be initially defined to determine how the model is expected to function. With the model defined a series of mathematical equations must be developed to describe the behaviour of the model. This includes the input data, the output data and the behaviour within the PVRO unit. With the mathematical model defined the unit can then be simulated and tested to determine whether the behaviour follows the behaviour of the real world PVRO system.

Mathematical Modelling - The Simplified Model

For the modelling of the PVRO unit the basic system is broken down into its base components. The PV array, the MPPT regulator, the battery, the inverter and the RO unit. This simplifies the modelling process as each component will have its own set of parameters that can be used to simulate the components contribution to the system. This breakdown of components is to be referred to as "The Simplified Model".

The PV array is on a fixed tilt and orientation wherein all cabling, soiling and tolerances are summarized into a single "percentage loss" value, the cell temperature derating is to be follow the ambient temperature and the derating factor and the panel power output is to be directly proportional to the global irradiance. The MPPT regulator is to have a fixed efficiency rating wherein the output is directly proportional to the input of the regulator from the PV array, the MPPT has a small idle drain that contributes to the idle power drain.

The battery energy flows similarly are assumed to have a fixed charge/discharge efficiency to account for any losses from the charging or discharging of the lead acid battery with the BMS contributing a small amount to the idle power drain. The inverter is assumed to have a fixed efficiency value and a significant idle drain that is to be added to the idle power drain.

The MPPT regulator, battery and inverter share a common DC bus and due to the short, heavy duty cable connecting them the DC voltage is assumed to be equal. In the simplified model of the electrical system MPPT regulator injects current into the DC bus, the Inverter draws current from the difference is to be either drawn from or injected from the battery as it charges or discharges.

The RO unit is assumed to be in either a running or idle state. In the running the state the unit is to be maintaining a fixed power draw while processing water at a fixed rate. In the idle state the unit is considered to have a smaller idle power drain from the control system in addition to the MPPT, BMS, inverter and other auxiliary power drains. The unit switches between the running and idle states depending on the battery SOC. If the battery goes above a "High" threshold it starts running and if the battery falls below a "Low" threshold the unit stops running and sits in an idle state.

The unit runs through a flushing sequence once it is told to shut down, this would add additional complexity to the simplified model of the system and hence is ignored as the simplified model only considers the unit to be either "running" or "idle".

Mathematical Modelling - Overview

Mathematical modelling of the PVRO system utilizes an iterative calculation method wherein the continuous operation of the unit is broken down into discrete 15-minute intervals. The model consists of input data which drives the model, the weather data is the only external input to the model and then a series of fixed input parameters allow adjustments of the model behaviour. This input data is fed into a series of equations that represent the PVRO system and the resultant output is the expected behaviour of the PVRO unit including the expected volume output of permeate water.

Mathematical Modelling - Inputs

The input weather data must be 15-minute interval data across a standard year and this data must be local to where the PVRO unit is expected to operate. This can be achieved in two ways, either directly through a weather station that has recorded 15-minute interval data or indirectly through applying daily recorded values and a standard 15-minute solar profile.

Directly obtaining 15-minute interval data for any given site is difficult without a dedicated local weather station but would provide the most accurate data for the mathematical model. The alternate approach is indirectly as it is more common for a given site to instead have daily irradiance values and then to assume a fixed standard solar profile such as a sine curve to convert the daily irradiance values into 15-minute interval data for the mathematical model. In either case it is preferable that the weather data is based on a ten to twenty-five year average to remove any unusual weather data that may be present within a single year of data.

The fixed input parameters are the key to the specific PVRO unit that is being modelled and are expected to change for different PVRO unit configurations. These key parameters are broken down into PV array, the MPPT regulator, the battery, the inverter and the RO unit. The PV array parameters are the rated solar capacity, the array tilt and array azimuth. The MPPT regulator parameters are the MPPT efficiency and the max current, MPPT voltage is assumed to equal the battery voltage. The battery parameters are the battery voltage, capacity and efficiency values. The inverter parameters are the inverter efficiency, which is assumed to be a fixed value rather than an efficiency curve and the inverter rating is assumed to always be greater than the load rating. The RO unit parameters are the running power, idle power, permeate output flowrate and the battery SOC high-low setpoints for switching the unit on or off. The RO unit is assumed to have fixed running power and permeate output flow rates regardless of water quality.

Mathematical Modelling - Equations

The energy calculations are based on the coulomb counting method where the current flows are calculated and used as the base for net energy flow over the 15-minute intervals. The equations use a discrete iterative method where values from the previous iteration to calculate each subsequent value. Each of the base components from the simplified model has its own set of energy equations that contribute to the simulation of the system.

The PV array equation inputs the weather data and the PV input parameters to calculate the effective array output in Watts. The equation utilises daily insolation data and the reference PV

profile to determine the effective irradiance at each interval. This is multiplied by the array rated power and the losses to output the output PV power for that interval.

$$PV\ Power_t = Daily\ Insolation * PV\ Profile_t * Array\ Rating * (1 - Losses)$$

The MPPT equations use the PV array output, the battery voltage and the MPPT input parameters to calculate the available current output of the MPPT regulator in Amps.

$$MPPT\ Current_t = \frac{PV\ Power_t * MPPT\ Efficiency}{Battery\ Voltage_t}, MPPT\ Current_t \leq MPPT\ Max\ Current$$

The Battery equations use the MPPT output current, the inverter input current and the battery input parameters to calculate the net battery current in amps. The net battery current is then used to calculate the battery SOC which is in turn used to calculate the new battery voltage in Volts.

$$Battery\ Current_t = (MPPT\ Current_t - Inverter\ Current_t) * Battery\ Efficiency$$

$$Battery\ SOC_t = \left(\frac{Battery\ Current_t}{Battery\ Capacity}\right) + Battery\ SOC_{t-1}, 0 \leq Battery\ SOC_t \leq 1$$

$$Battery\ Voltage_t = (0.85 + (Battery\ SOC_{t-1} * 0.275) * Rated\ Battery\ Voltage$$

The Inverter equations use the load power, the previous battery voltage and the Inverter input parameters to calculate the inverter input current in Amps.

$$Inverter\ Current_t = \frac{Load\ Power_t}{Battery\ Voltage_t * Inverter\ Efficiency}$$

The RO equations use the battery SOC and the previous running state to determine the current running state, emulating the on/off decision behaviour of the battery monitor unit. Once the current running state is determined the input parameters define the current load power in Watts. To determine the net permeate water output the operating hours of the unit are summed and multiplied by the input parameter for permeate output flowrate to get the total water output in litres.

$$if\ (Running\ State_{t-1} == True\ \&\ Battery\ SOC_{t-1} < Off\ Setpoint)\ , Running\ State_t = False$$

$$if\ (Running\ State_{t-1} == False\ \&\ Battery\ SOC_{t-1} > On\ Setpoint)\ , Running\ State_t = True$$

$$if\ (Running\ State_t == True\ )\ , Load\ Power_t = RO\ Running\ Power$$

$$if\ (Running\ State_t == False\ )\ , Load\ Power_t = RO\ Idle\ Power$$

$$if\ (Running\ State_t == True)\ , Permeate\ Output_t = Rated\ Output$$

The equations become interdependent with calculations for current values of one equation depending on the previous values from the other equations. This becomes a reasonably accurate emulation of the real-world system as all components within the PVRO system are also interdependent and have an influence on the PVRO unit behaviour.

Mathematical Modelling - Simulation

Microsoft Excel is used to handle the iterative calculations wherein a year of operational data is produced from localised weather data and the set of fixed input parameters. All the fixed input parameters are accessible from an "Input Parameters" sheet to allow easy access to these variables and quick alterations to be made.

The weather data is input across two sheets, one for the 15-minute profile data and one for the monthly data values. This data is later used to calculate the 15-minute weather data for the simulated year.

The equations are implemented within each 15-minute interval to calculate the operational data of the unit at that specific time. The model does this for every 15-minute interval across a year with each month separated into its own data sheet for easy navigation of the raw data.

The raw data is summarised within a "Output Data" sheet with each month data summarised and a typical operational day is shown in a graph. The goal of the PVRO system is to produce clean permeate water output hence the key output parameter highlighted is the total volume of water for each month and the total for the year.

Initially the model must be compared with the real-world system to determine the models accuracy and to compensate for any errors obtained. To accommodate this the data obtained from the PVRO unit monitoring system is collected.

A large volume of data is required with the unit running to obtain a reasonable snapshot of the unit operation and to overcome any atypical operation of the unit that may arise through abnormal weather or external influences. This data can then be placed alongside the simulated data for the same time period for easy comparison between the simulated and real-world systems.

Mathematical Modelling - Analysis

With the comparison complete and any necessary compensation made to the model the simulation can then be utilised to predict how the unit would behave in alternate configurations or scenarios. By altering the fixed input parameters and monitoring the output data it is easy to see the effects of changing one of the components such as the PV array size or the battery size to determine the effects on the PVRO unit net permeate output. By replacing the weather data with weather data from an alternate location it can be determined how the same unit would perform in various locations. By replacing all the RO unit input parameters, different size RO unit performance could be estimated to some degree.

Results

The results of this project are split into the two stages of the project, the preliminary and the refined results. In the preliminary results section, the simulated data is relying on the base assumptions for the input parameters of the Excel simulation. These results are then compared with the data from the PVRO monitoring system to compare the simulation with real world system. In the refined results section, the simulation is using the comparison from the preliminary results with the measured data to fine tune the input parameters. With the input parameters adjusted the refined results are compared with the real-world system to assess the performance of the mathematical model.

Preliminary

Preliminary – Simulated Data

Preliminary simulation data required some of the input parameters to be assumed while the remaining data was collected from the relevant datasheets. For the solar array, the panel rating was known to be 370W, number of panels in the array is 12 and array tilt were known as 30-degrees beforehand. Similarly, the 48V 100Ah AGM information was added to the input parameters with the battery efficiency assumed based on similar batteries [28]. The MPPT regulator and AC Inverter information was collected from their appropriate datasheets including ratings and max efficiency [29] [30]. The PVRO unit is rated for 500L/hr, the running load power, idle load power and setpoints were estimated based on information from Moërk water solutions. A summary listing the preliminary input parameters used is shown in the table below.

Solar Capacity	4440 Watts
Panel Tilt	30 Degrees
Longitude	31.7 Degrees
MPPT Max Current	70 Amps
Battery Capacity	100 Amp-Hours
Battery Voltage	48 Volts
On Setpoint	90% SOC
Off Setpoint	75% SOC
RO Unit Running Power	2500 W
RO Unit Idle Power	50 W
Permeate Output Flowrate	500 L/hr
Solar Losses	5%
MPPT Efficiency (peak)	99%
Inverter Efficiency (peak)	95%
Battery Efficiency	97%

Table 1: PVRO Simulation Preliminary Input Parameters

The output data from the simulation was collected for two sample months, March and May. Each month had the operation data averaged and summarised into a typical operational day. The two graphs below represent this operational data for the preliminary simulated PVRO system for the months of March and May.
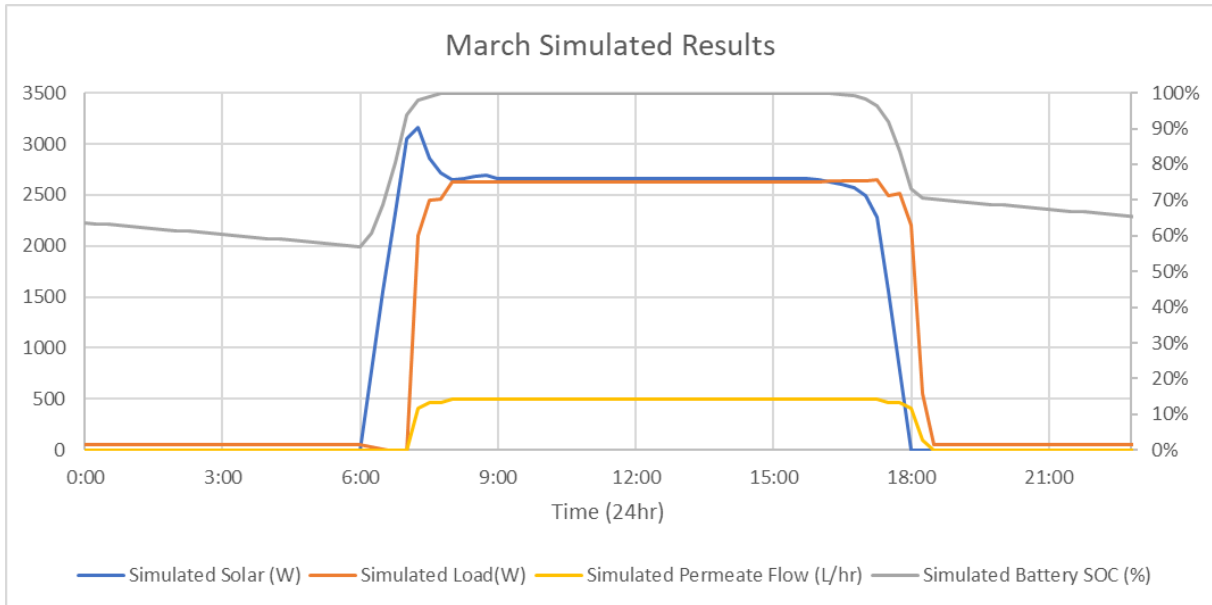
Figure 18: March Preliminary Siulated Results Graph

In the preliminary simulated results for the month of March, the graph illustrates the typical daily operational data for the simulated PVRO system. First looking at the solar array input power the power quickly picks up in the morning until the battery SOC hits 100% where the input solar power cuts back as once the battery is charged the solar array is directly powering the RO unit load power. The simulated load power follows the expected behaviour, drawing a small idle power overnight until in the morning the battery SOC rises above the ON threshold and the unit powers up, drawing the full RO unit running load power. The permeate flow profile mimics the on off behaviour of the with the expected 500L/hr while running and stopping when the unit is idle. The battery SOC drops gradually overnight as the idle power drains the battery but quickly rises to 100% once the morning solar power picks up and the battery is charged.
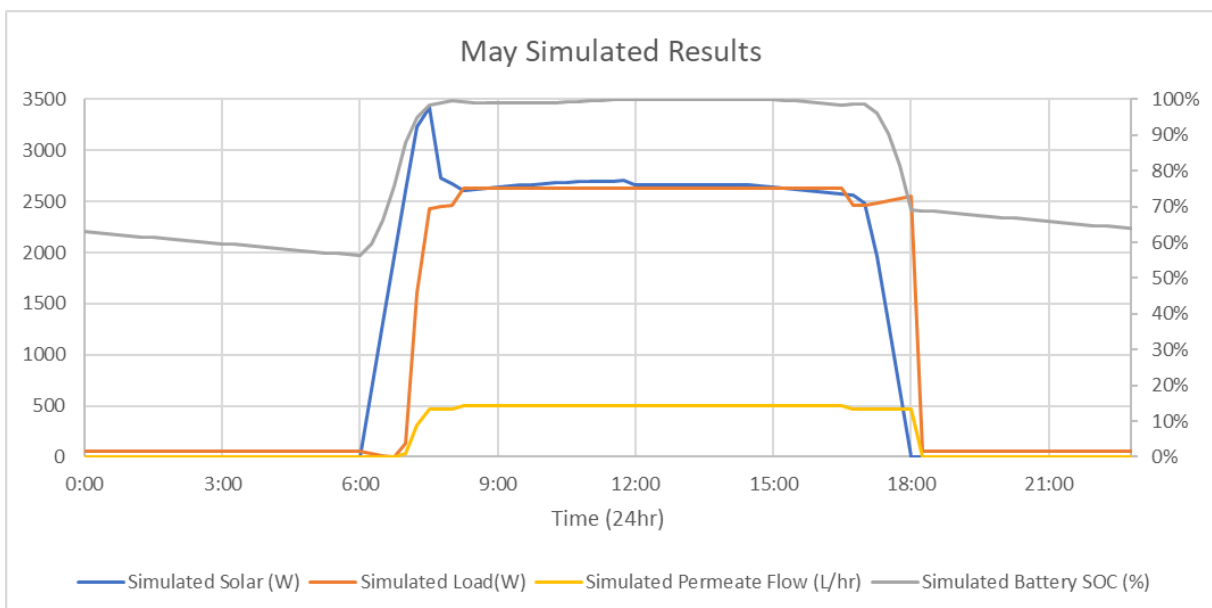

Figure 19: May Preliminary Simulated Results Graph

The graph for the preliminary simulated May operational data shows almost identical behaviour to that of the preliminary simulated March graph. The one minor difference between the two is the May graph has less operational hours than the March data. The simulated PVRO unit takes longer to start-up in the morning due to less solar power being available. This is expected as the solar power availability in the winter months is less than the autumn months. Both simulated graphs demonstrate the PVRO simulation is outputting the expected 'ideal' PVRO system behaviour.

Preliminary – Monitoring Data

The data from the monitoring system was collected and analysed. Two months of data were collected as sample data for the system, March and May. Some data points for these two months were missing, to remedy this the results were interpolated using the adjacent data to fill in the gaps making it easier to compare the data with the simulated data. For each of the two months the operational data was then averaged and summarised into a typical operational day. The two graphs below represent this operational data for the monitored Muresk PVRO unit.
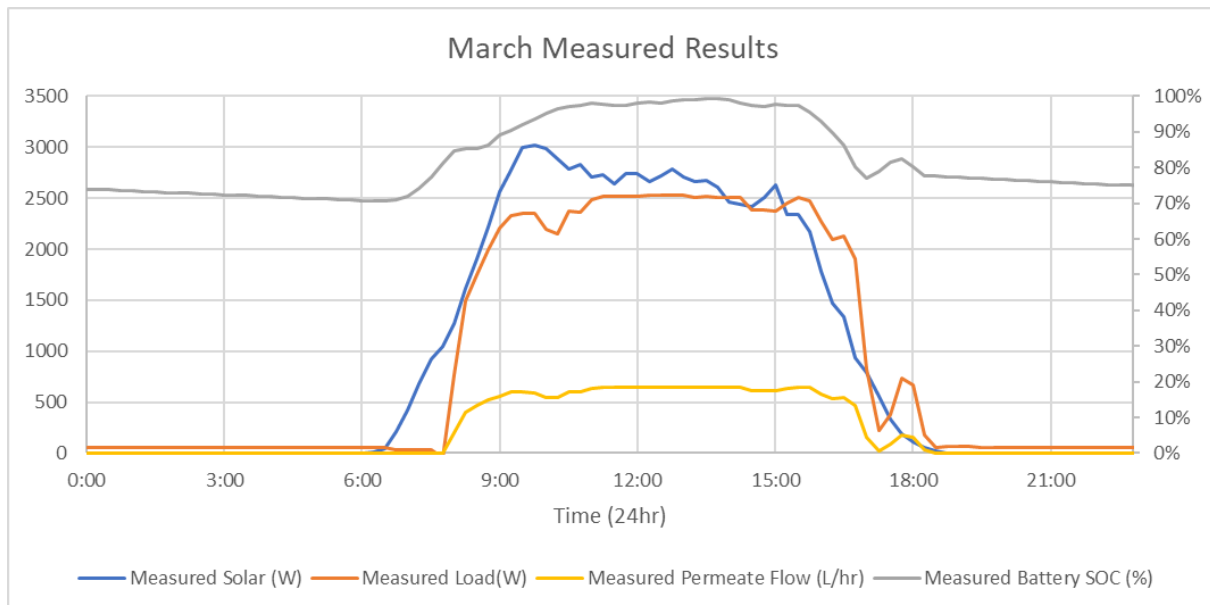

Figure 20: March Preliminary Measured Results Graph

In the measured results from the PVRO system for March, the graph represents what the real-world operational data for the system on an average day in March. The measured solar shows the utilised solar power is operating as expected, picking up in the morning, then backing off when the battery SOC approaches 100%. The solar power is less stable than in the simulated results, most likely due to minor variations in the available solar energy from cloud activity. This variation seems to have an impact on the measured load power with instability in the average load power appearing when the unit switches on and off due to some sample days experiencing high variations in cloud cover. The variation in load power is reflected in the permeate flow with the average data showing instability in the output from the unit switching on/off on some of the sample days. One notable difference is the permeate output appears higher than the simulated data graph, this could be due to the unit performing higher than expectations or the flow meters not being calibrated correctly. Also the

battery SOC appears to peak just below 100%, this could be due to the averaging of the data picking up sample days where the solar power is insufficient and lowering the average.
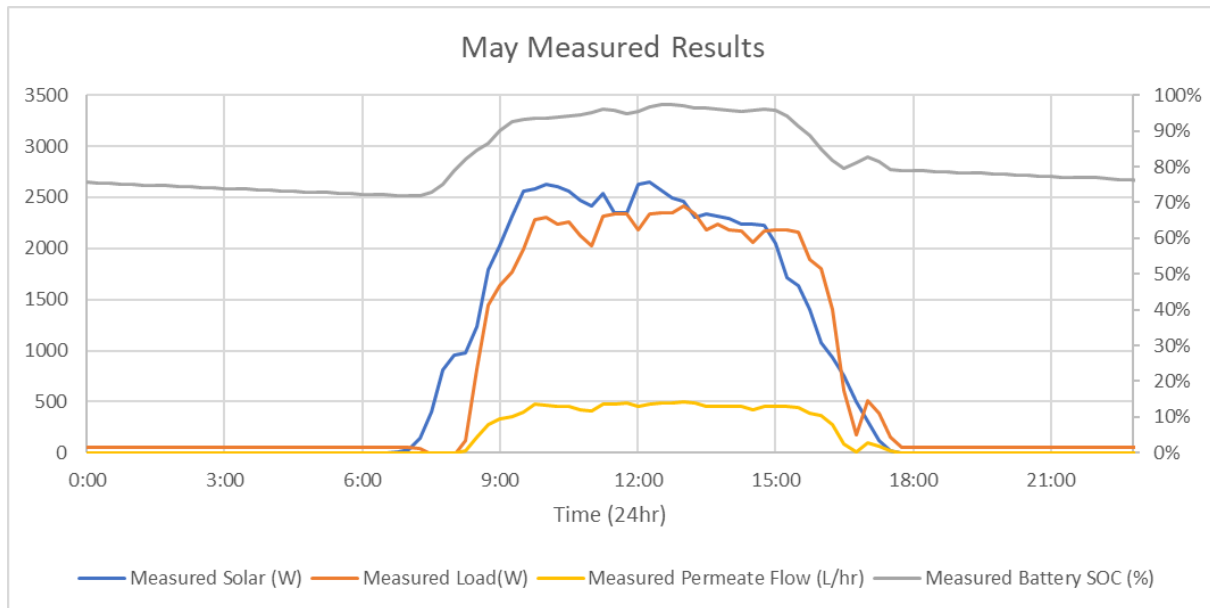

Figure 21: May Preliminary Measured Results Graph

The graph for the measured May PVRO system operational data has similar behaviour to that of the March graph but shows more instability indicating there were more days where the cloud cover was impacting the operation of the unit. This is expected as the further into winter it is typical to have less available solar and higher chances of cloudy days. The measured solar power shows both these aspects with general instability, a later peak in power in the morning and faster drop-off in the afternoon. The RO unit load power and permeate flow shows this behaviour as well but to a lesser degree with the battery soaking up some of these changes but the unit's average operation time appears to be reduced from March.

Preliminary – Comparison

Tuning of the excel model requires several key parameters to be compared and adjustments made in order to compensate for the variances between the measured data and the simulated data. The RO idle load power and running load power can be directly adjusted by setting their corresponding input parameters to match the measured RO power data. The next key parameter is the input solar power which is measured by summing the total kWh from an average day for each month. Adjustments are made by modifying the solar losses input parameter. The final key parameter is the daily permeate which is the total output of product water from the RO unit for an average day from each month.

	Idle Load (W)	Running Load (W)	Solar Daily (kWh)	Daily Permeate (L)
Measured	50.1	2457.4	23.1	5470.9
Simulated	50.0	2500.0	29.8	5445.3
Error %	-0.1%	1.7%	28.9%	-0.5%

Table 2: March preliminary model comparison of key parameters

First looking at the key parameter comparison for the month of March, most parameters from the simulated data appear to closely follow their corresponding measured data parameters. The idle load was measured by averaging the load power during the night when the unit was idle, this shows an error of just 0.1% indicating the initial idle load parameter of 50W was very close. Similarly the running load which was measured by averaging the load power during the day while the unit was running, showing an error of just 1.7% also very close to the initial running load parameter of 2500W. The solar daily kWh parameter shows a significantly higher error of 28.9% above the measured value, indicating the simulation is overstating the available solar energy. The daily permeate volume shows a surprisingly low error of 0.5% despite the significant error in the solar daily kWh parameter.

	Idle Load (W)	Running Load (W)	Solar Daily (kWh)	Daily Permeate (L)
Measured	49.8	2264.6	18.8	3484.0
Simulated	50.0	2500.0	29.4	5390.6
Error %	0.4%	10.4%	56.9%	54.7%

Table 3: May preliminary model comparison of key parameters

Then looking at the key parameter comparison for the month of May, there seems to be significantly higher errors in the key parameters than the month of March. The idle load parameter is reasonably close with only 0.4% error, but the running load parameter has an increased error of 10.4% indicating the simulation is overstating the power consumption of the RO unit. The solar daily kWh value shows even higher error than the month of March with an error of 56.9% more than the measured value, the model is significantly overstating the available solar daily energy. The daily permeate also shows a significant error of 54.7% more than the measured value, some of this error could be linked to the running load power and solar daily kWh errors.

To reduce the errors seen between the simulated and measured key parameters the simulation input parameters need to be adjusted. The errors from the two months are averaged then used to adjust the simulation input parameters. Since the solar daily kWh parameter is influence by the two load power parameters and the daily permeate parameter is influenced by all three parameters the parameters will need to be adjusted sequentially to minimise the final errors. These adjusted values were then used in the final simulation for the detailed analysis of the model.

Refined Results

Refined Results – Adjusted Model

The refined results use the adjusted parameters from the preliminary model comparison. During the tuning process there was significant errors with the solar daily kWh and the daily permeate output. The model appears to be overstating the available solar energy and hence the solar losses were set to 20% in attempt to compensate. The daily permeate showed similar error but only for the May preliminary simulated data, the March preliminary simulated date was much closer and hence was decided to keep the default permeate flowrate parameter the same. The adjusted simulation input parameters are shown in the table below:

Solar Capacity	4440 Watts
Panel Tilt	30 Degrees
Longitude	31.7 Degrees
MPPT Max Current	70 Amps
Battery Capacity	100 Amp-Hours
Battery Voltage	48 Volts
On Setpoint	90% SOC
Off Setpoint	75% SOC
RO Unit Running Power	2361.0 W
RO Unit Idle Power	49.9 W
Permeate Output Flowrate	507.5 L/hr
Solar Losses	20%
MPPT Efficiency (peak)	99%
Inverter Efficiency (peak)	95%
Battery Efficiency	97%

Figure 22: PVRO Simulation Refined Input Parameters

Minor adjustments were made to the RO unit idle power consumption and the RO unit running power consumption parameters to reduce the overall errors. The solar losses was increased to compensate for the simulation overstating the available solar energy. Due to the large variations between the preliminary March and May key parameters it is not expected that these changes will improve the errors for both months.

	Idle Load (W)	Running Load (W)	Solar Daily (kWh)	Daily Permeate (L)
Measured	50.1	2457.4	23.1	5470.9
Simulated	49.9	2361.0	27.9	5471.0
Error %	-0.3%	-3.9%	20.7%	0.0%

Figure 23: March refined model comparison of key parameters

Looking at the March adjusted model key parameters, the errors appear to be like the preliminary March key parameters. The RO idle load power and the RO running load power errors have been marginally increased due to the changes. The solar daily kWh has been improved but still significant error remains with the simulated data overstating the available solar power. The daily permeate output changes eliminated the error.

	Idle Load (W)	Running Load (W)	Solar Daily (kWh)	Daily Permeate (L)
Measured	49.8	2264.6	18.8	3484.0
Simulated	49.9	2361.0	27.3	5368.4
Error %	0.2%	4.3%	45.8%	54.1%

Figure 24: May refined model comparison of key parameters

The May adjusted model key parameters all show improvements from the preliminary May key parameters. There is improvement in the RO idle and running load parameters with the errors approximately half what they were in the preliminary data. The solar daily kWh parameter has improved marginally but still significantly overstating the available solar energy. The daily permeate output also shows almost no improvement, still overstating the permeate output.

From this it is apparent that deeper analysis, comparing the modelled data with the monitoring data is required to improve the model further.

Refined Results – Simulation Output

Using the model to simulate this system over the course of a year gives important insights into how the system behaves throughout the year. This data is summarized into three graphs showing the solar utilization of the system, the monthly min/max battery SOC and the average daily water production. The irradiation data for 2019 was added to the simulation to see how the PVRO unit would behave across the sample year.
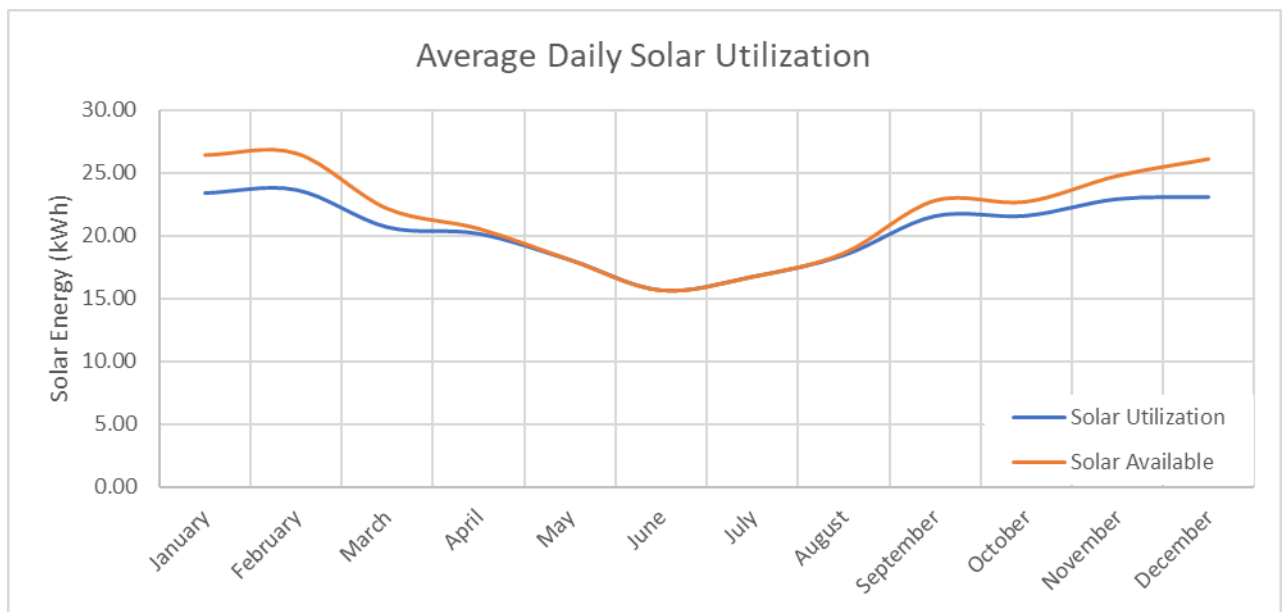

Figure 25: 30-degree tilt average daily solar utilisation graph

The average daily solar utilization shows how much power the PVRO unit is consuming vs the available solar energy for an average day for each month of the year. This data can be used to determine how the array size and tilt can be adjusted to maximise the solar utilization for every month across the year. In the sample year the array is showing an excess of solar energy in the summer months and a shortage of the winter months. The net solar utilization for the sample year with the standard configuration is 7494kWh.
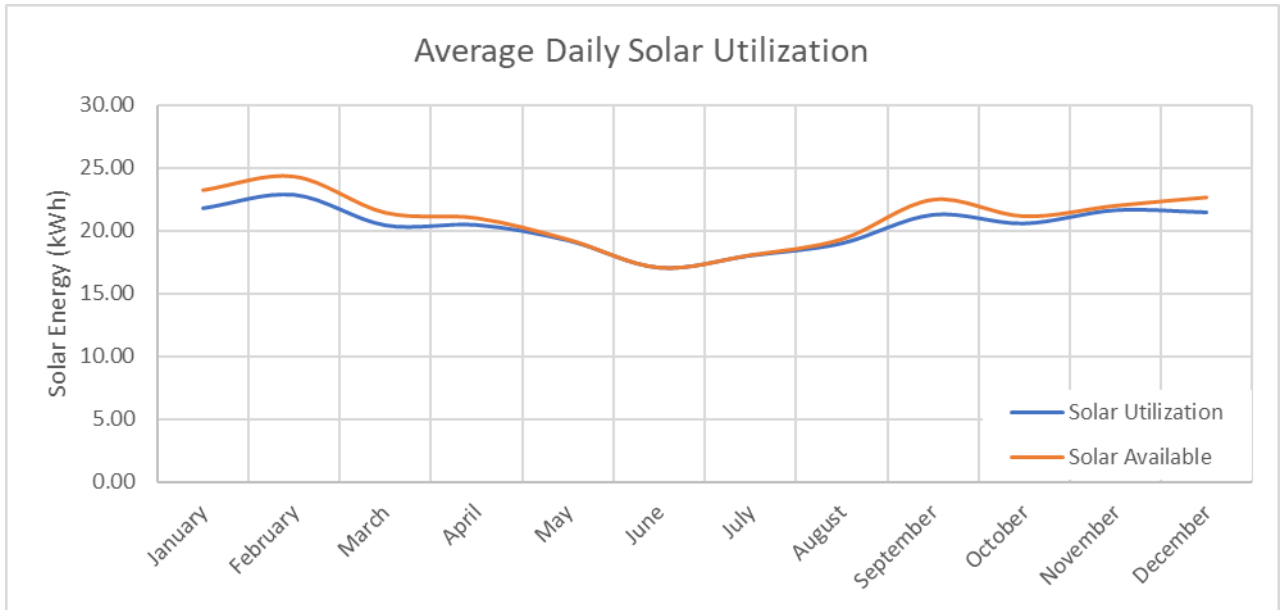
Figure 26: 45-degree tilt average daily solar utilisation graph

By simply adjusting the array tilt from 30 degrees to 45 shows an increase in the winter utilization with minimal impact on the utilization during the summer months. The net solar utilization for the year has reduced slightly to 7413kWh but has improved the consistency of the utilization throughout the year. Potentially increasing the tilt angle further and increasing the solar array size could improve the solar utilization throughout the year.
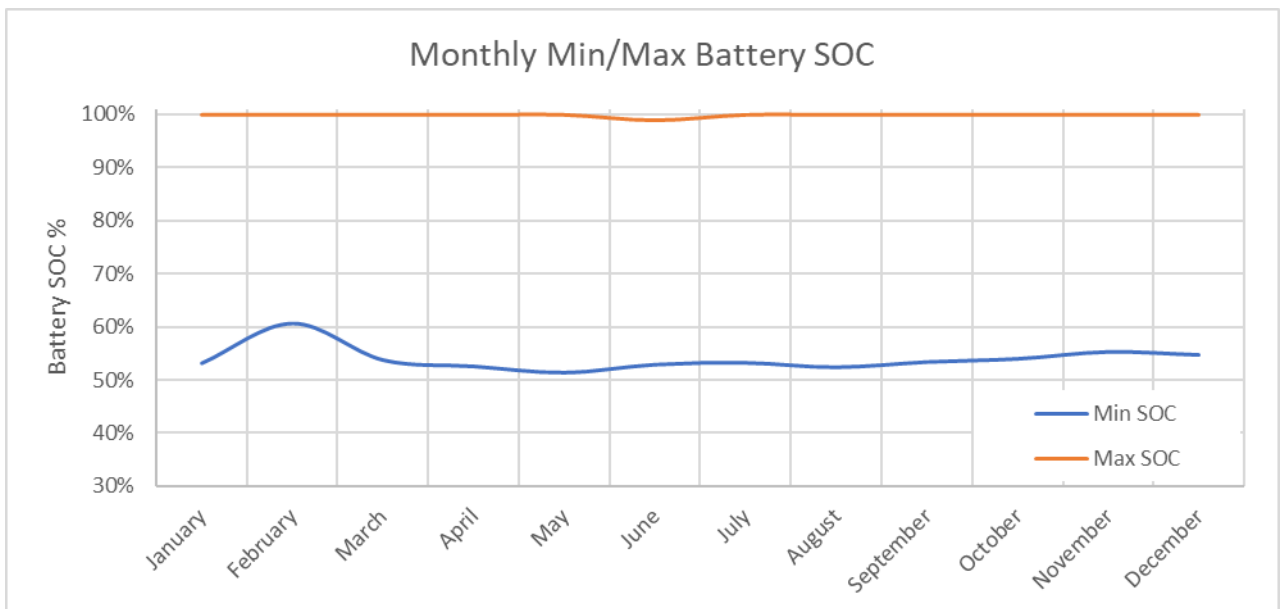

Figure 27: Refined results monthly min/max battery SOC graph

Next the monthly min/max battery SOC gives an insight into how hard the battery is working. If the max battery SOC dips below 100% it indicates the solar array is insufficient to fully charge the battery during the day and may be undersized. Looking at the sample year there is a slight dip in

June indicating the battery was not fully charged during that month and the solar array may be undersized. Similarly the min battery SOC indicates the lowest SOC the battery got to, if this drops too low the system my unexpectedly shut down and require manual restart. In the sample data the SOC never drops below 50% so the battery is sufficiently sized to handle the overnight idle loads safely.
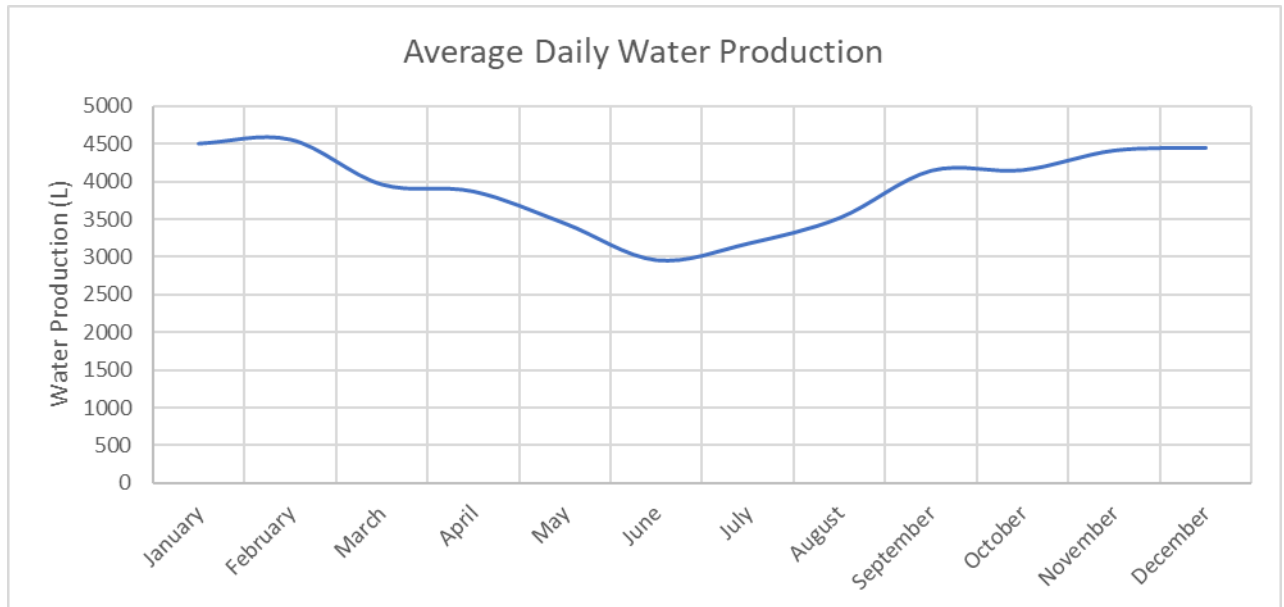

Figure 28: 30-degree tilt average daily water production graph

Finally, the average daily water production shows what the PVRO unit would typically produce on an average day for each month. This is the key performance for the data as it indicates how much water the unit can produce throughout the year. In the sample year the unit follows a similar trend to the solar utilization, with significantly higher production in the summer months than the winter months. There appears to be due to the lack of solar energy in the winter months limiting the operation hours of the PVRO unit. Under the standard configuration the unit would produce 1,451,576L of permeate water for the sample year
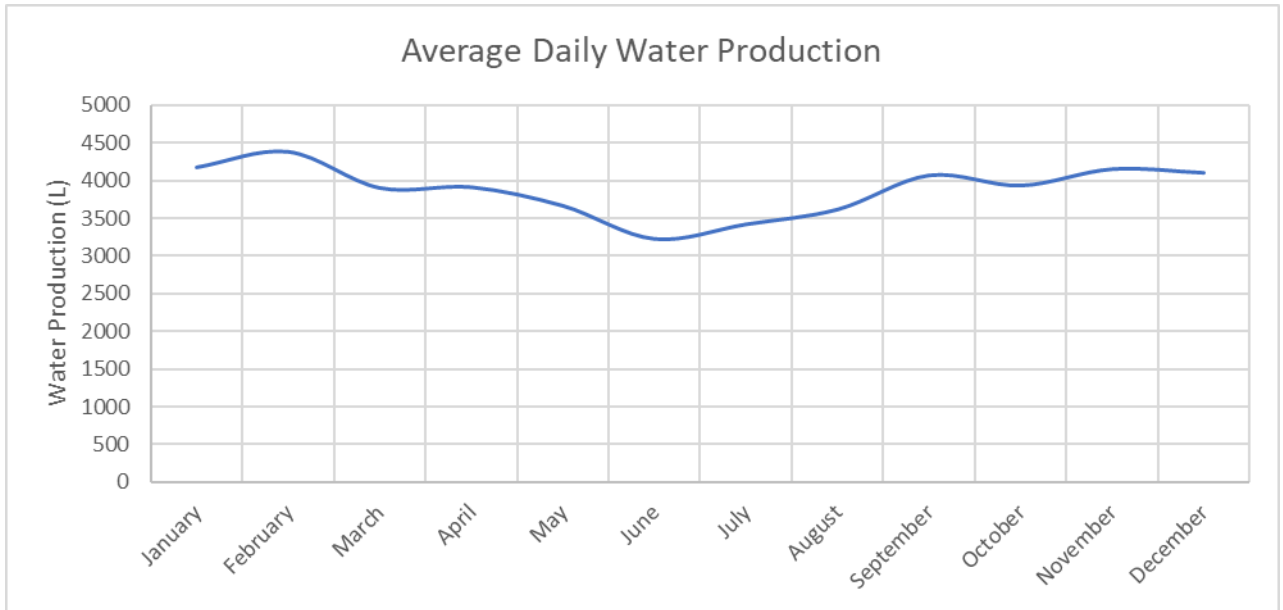
Figure 29: 45-degree average daily water production graph

If we again change the array tilt from 30 degrees to 45 degrees, we see a significant increase in water production in water production in the winter months and a minor drop in production in the winter months. The net water production for the sample year is now 1,435,971L, a minor drop in total output but the unit's performance across the year is more consistent under this configuration.

Discussion

Looking at the variations in errors seen between the May and March data, it is apparent there are still significant errors in the model. This may be due to the variations in the conditions between the two sample months. However, coupled with the significant error in the solar data it is more likely an error in the mathematical model. There are also limitations in the accuracy of the monitoring data that may be contributing to the errors seen. These includes the flow sensors and AC current sensors being uncalibrated. More data and a deeper analysis are required to find the source of this error and to improve the accuracy of the mathematical model. Additional sensors for the monitoring system would also aid in finding the source of errors. including irradiance sensors to allow direct validation of the solar data. Otherwise the model demonstrates it's potential, matching the typical behaviour of the Muresk PVRO unit.

The key output of the simulation is the permeate water production. Knowing how much water the unit would produce on different days of the year and the net output of the year helps match the PVRO unit to its target application. Changing the tilt of the array to a steeper angle for example improves the consistency of the output throughout the year, which is important where a minimum daily output is required. In contrast keeping a shallower angle is better for maximising the total annual output of the unit. In this regard the true optimisation is more dependant on the intended purpose of the PVRO unit than a single output metric.

Conclusion

In this project a monitoring system has been successfully developed to log the operational data of the Muresk PVRO unit utilizing an Arduino based monitoring system and an IOT portal. From this data a basic mathematical model was developed and implemented using Microsoft Excel.

The validation and tuning of the model were partially achieved with a model that follows the base behaviour of the unit, but with limited accuracy. To better validate the simulation of the solar component a local irradiance and temperature sensor would provide greater insights and allow for a more direct comparison of the model against the monitored data. Similarly adding additional sensors to monitor the AC power draw and calibration of the water flow sensors would increase the accuracy of the model by removing uncertainties in the measured data and provide a better baseline for comparison. The model itself could also incorporate the PVRO units flushing behaviour by real-time monitoring of the unit during a typical cycle, this would improve the model by allowing for the additional power load drawn during this time, rather than ignoring this behaviour.

This project demonstrates the potential for optimisation through the mathematical model. By adjusting parameters under a virtual environment, effects of individual changes can be assessed prior to making changes in the real world PVRO system. For the model to become more accurate and more useful it requires further improvements through more extensive data acquisition and analysis. Currently the project is relying on two months of data to calibrate the model. The variance between the two months demonstrates the insufficiency of this data. More data throughout the year would allow for a better average and a better profile for the summer and winter months to validate the varying seasonal behaviour.

Once the behaviour for the pilot PVRO unit is sufficiently modelled and validated, the opportunity to expand this simulation to other PVRO units of different scales is possible. Additionally, by altering the climate data, the PVRO unit can be tested in alternate locations across the world. Potential improvements could be made and analysed in locations which have less available solar resource or situations which require higher permeate outputs for certain times of the year.

The analysis and optimisation through mathematical modelling for the Muresk farm photovoltaic reverse osmosis treatment plant project has demonstrated that potential, future work on this project could lead to further insights into the behaviour of this system and the potential for future optimisation and applications.

Recommendations

Future improvements can be made to this project to ensure higher accuracy of both the monitoring system and the mathematical model. Tuning of the flow sensors and current sensors will ensure all the accuracy obtained be the monitoring system. Adding additional sensors in the form of a local weather station would provide more data and coupled with long term data acquisition, would give the necessary information required to properly tune and validate the mathematical model.

The mathematical model should be properly tuned using extended monitoring data. The model needs to be improved by improving the accuracy of the solar data including finding the source of the overstating error and improving the solar profile to properly account for summer winter variations. Accuracy can be further improved by adding the RO flushing sequence into the simulation to account for the power loss during this cycle.

References

[1] B. Wu, A. Maleki, F. Pourfayaz and M. A. Rosen, "Optimal design of stand-alone reverse osmosis desalination driven by a photovoltaic and diesel generator hybrid system," *Solar Energy,* vol. 163, pp. 91-103, 2018.

[2] P. Kalt, C. Birzer, H. Evans, A. Liew, M. Padovan and M. Watchman, "A Solar Disinfection Water Treatment System for Remote Communities," *Procedia Engineering,* vol. 78, pp. 250-258, 2014.

[3] J. Song, T. Li, L. Wright-Contreras and A. W.-K. Law, "A review of the current status of small-scale seawater reverse osmosis desalination," *Water International,* vol. 42, no. 5, pp. 618-631, 2017.

[4] L. F. Greenlee, D. F. Lawler, B. D. Freeman, B. Marrot and P. Moulin, "Reverse osmosis desalination: Water sources, technology, and today's challenges," *Water Research,* vol. 43, pp. 2317-2348, 2009.

[5] J. Cutrova, N. Voutchkov, J. Fawell, P. Payment, D. Cuncliffe and S. Lattemann, "Desalination Technology: Health and Environmental Impacts," Taylor & Francis Group, LLC, Boca Raton, 2011.

[6] V. V. Tyagi, N. A. A. Rahim, N. A. Rahim and J. A. L. Selvaraj, "Progress in solar PV technology: Research and achievement," *Renewable and Sustainable Energy Reviews,* vol. 20, pp. 443-461, 2013.

[7] M. A. Green, E. D. Dunlop, D. H. Levi, J. Hohl-Ebinger, M. Yoshita and A. W. Ho-Baillie, "Solar cell efficiency tables (version 54)," *Progress in photovoltaics,* vol. 54, pp. 565-575, 2019.

[8] D. Kurz, K. Lewandowski and M. Szydłowska, "Analysis of efficiency of photovoltaic bifacial cells," in *ITM web of confenerences 19*, Poznan, 2018.

[9] S. N. R. Kantareddy, I. Mathews, S. Sun, M. Layurova, J. Thapa, J.-P. Correa-Baena, R. B. T. Buonassisi, S. E. Sarma and I. M. Peters, "Perovskite PV-powered RFID: enabling lowcost self-powered IoT sensors," *IEEE Sensors Journal,* vol. 1, no. 1, 2019.

[10] S. Comello, S. Reichelstein and A. Sahoo, "The road ahead for solar PV power," *Renewable and Sustainable Energy Reviews,* vol. 92, pp. 744-756, 2018.

[11] S. Kumarasamy, S. Narasimhan and S. Narasimhan, "Optimal operation of battery-less solar powered reverse osmosis plant for desalination," *Desalination,* vol. 375, pp. 89-99, 2015.

[12] H. Keshan, J. Thornburg and T. S. Ustan, "Comparison of Lead-Acid and Lithium Ion Batteries for Stationary Storage in Off-Grid Energy Systems," Electrical Engineering Department, PEC University of Technology, Chandigarh.

[13] R. I. S. Pereira, S. C. S. Juca and P. C. M. Carvalho, "IoT embedded systems network and sensors signal conditioning applied to decentralized photovoltaic plants," *Measurement,* vol. 142, pp. 195-212, 2019.

[14] S. M. Patil, V. M and R. Tapaskar, "IoT based Solar Energy Monitoring System," in *International Conference on Energy, Communication, Data Analytics and Soft Computing*, Hubballi, 2017.

[15] A. Lopez-Vargas, M. Fuentes and M. Vivar, "IoT Application for Real-Time Monitoring of Solar Home Systems Based on Arduino With 3G Connectivity," *IEEE Sensors Journal,* vol. 19, no. 2, pp. 679-691, 2019.

[16] K. J. Singh and D. S. Kapoor, "Create Your Own Internet of Thing: A survey of IOT platforms," *IEEE Consumer Electronics Magazine,* pp. 57-68, 2017.

[17] B. Nakhuva and T. Champaneria, "Study of Various Internet of Things Platforms," *International Journal of Computer Science & Engineering Survey,* vol. 6, no. 6, pp. 61-74, 2015.

[18] D. Brunelli, C. Villani, D. Balsamo and L. Benini, "Non-invasive voltage measurement in a three-phase autonomous meter," *Microsyst Technol,* vol. 22, pp. 1915-1926, 2016.

[19] D. Porcarelli, D. Brunelli and L. Benini, "Clamp-and-Forget: A self-sustainable non-invasive wireless sensor node for smart metering applications," *Microelectronics Journal,* vol. 45, pp. 1671-1678, 2014.

[20] Victron Energy, "Victron Energy VE.Direct Protocol," [Online]. Available: https://www.victronenergy.com/support-and-downloads/whitepapers. [Accessed 10 November 2019].

[21] Victron Energy, "Victron Energy VE.Direct Protocol BlueSolar and SmartSolar MPPT chargers," [Online]. Available: https://www.victronenergy.com/support-and-downloads/whitepapers. [Accessed 10 November 2019].

[22] Victron Energy, "Victron Energy VE.Direct Protocol Phoenix Inverters," [Online]. Available: https://www.victronenergy.com/support-and-downloads/whitepapers. [Accessed 10 November 2019].

[23] Victron Energy, "Victron Energy BMV700 Series Hex Protocol," [Online]. Available: https://www.victronenergy.com/support-and-downloads/whitepapers. [Accessed 10 November 2019].

[24] R. C. Asher, "Ultrasonic sensors in the chemical and process industries," *Journal of Phisics E: Scientific Instruments,* vol. 16, pp. 959-963, 1983.

[25] T. Khatib and W. Elmenreich, "Novel simplified hourly energy flow models for photovoltaic power systems," *Energy Conversion and Management,* vol. 79, pp. 441-448, 2014.

[26] A. Ausswamaykin and B. Plangklang, "Design of Real Time Management Unit for Power Battery in PV-Hybrid Power Supplies by Application of Coulomb Counting Method," in *Proceedings of the International Electrical Engineering Congress* , Rajamangala, 2014.

[27] Y. Liu and S. M. Wang, "Design of Desalination Reverse Osmosis System Power-Supplied By PV and Wind Energy," *Applied Mechanics and Materials,* Vols. 541-542, pp. 961-965, 2014.

[28] G. Notton, C. Paoli, S. Vasileva, M. L. Nivet, J.-L. Canaletti and C. Cristofari, "Estimation of hourly global solar irradiation on tilted planes from horizontal one using artificial neural networks," *Energy,* vol. 39, pp. 166-179, 2012.